Title	Preparation of Ag/TiO₂ Composite Films by the Sol-Gel Method (Commemoration Issue Dedicated to Professor Sumio Sakka On the Occasion of His Retirement)
Author(s)	Kozuka, Hiromitsu; Zhao, Gaoling; Sakka, Sumio
Citation	Bulletin of the Institute for Chemical Research, Kyoto University (1994), 72(2): 209-224
Issue Date	1994-10-31
URL	http://hdl.handle.net/2433/77565
Right	
Type	Departmental Bulletin Paper
Textversion	publisher

Preparation of Ag/TiO₂ Composite Films by the Sol-Gel Method

Hiromitsu Kozuka*, Gaoling Zhao* and Sumio Sakka*

TiO₂ coating films containing dispersed, nanometer-sized Ag metal particles have been prepared by the sol-gel method using a starting solution containing $Ti(OC_3H_7^i)_4$ and $AgNO_3$ in a molar ratio of 1 : 0.062. When the gel films were exposed to formalin vapor at room temperature, reduction of Ag ions occurred, and the films exhibited intense yellow color and relatively sharp optical absorption at a wavelength of 441 nm, which is attributed to surface plasma resonance of Ag metal particles. TEM observation revealed formation of Ag metal particles of 4~23 nm in size in the gel films exposed to formalin vapor. Heat-treatment of the gel films at 600~800°C in air resulted in formation of anatase or rutile polycrystalline films of 0.26 μm in thickness containing dispersed Ag metal particles of 5~45 nm in size. The heat-treated films exhibited broad optical absorption ranging from ultraviolet to 1,000 nm. Formalin vapor exposure prior to heat-treatment, however, did not affect the microstructure and optical absorption characteristics of the heat-treated coating films.

KEY WORDS: Composites/ Metal particles/ Coating films/ Silver/ Titania/ Surface plasma resonance/ Sol-gel method

1. INTRODUCTION

Composite materials comprising metal nanoparticles and dielectric media are attracting much attention in the field of advanced materials of various optical functions. Surface plasma resonance of metal particles, which enhances the electric field of light inside and outside nearby the particles, is the most significant origin of the optical functions of these materials.[1] For instance, third order optical nonlinearity of metal is enhanced at surface plasma frequency by large electric field induced by light when the metal is in the form of nanoparticles.[2] It is also known that when dye molecules[3-5] or rare earth ions[6] are embedded with nanometer-sized metal particles in dielectric media, their fluorescence is enhanced at surface plasma frequency of the metal particles. In utilizing surface plasma resonance in optical functionality, the frequency or wavelength at which surface plasma resonance occurs and the resonance intensity should be controlled. This can be achieved by selecting appropriate metals and dielectrics and by controlling the size, shape and volume fraction of metal particles in the composites.

Sol-gel method has much advantage for preparing such composite materials.[8-13] Nanometer-sized metal particles can be precipitated in large volume fraction in homogeneous, amorphous oxide gel matrices, and formation and hence the size and/or shape of metal particles

* 幸塚広光, 趙 高凌, 作花濟夫 : Solid State Chemistry IV, Institute for Chemical Research, Kyoto University, Uji, Kyoto 611.

can be controlled through controlling the size of the gel pores and the structure of the gel networks. The present authors, in fact, have previously shown that in Au/SiO$_2$ composite coating films the size and shape of Au metal particles are greatly affected by several sol-gel preparation parameters such as the amount of water used for hydrolyzing silicon alkoxide and the sol-aging time.[8,9] Another advantage of the sol-gel method is that it can make transparent coating films of various polycrystalline oxides. Because the dielectric constant of dielectric media is one of the determining factors for surface plasma resonance, employing and examining various oxide crystals as matrices for metal particles are challenging for making new optical materials.

Pt and Pd nanoparticles are known to exhibit optical absorption in ultraviolet region when embedded in conventional oxide glasses. In previous works[9,11] we have prepared TiO$_2$ coating films containing dispersed, nanometer-sized Pt and Pd metal particles that show broad optical absorption in the visible range, utilizing the effect of dielectric matrices with higher dielectric constants, which shift surface plasma resonance towards longer wavelengths. In the present work, TiO$_2$ coating films containing dispersed, nanometer-sized Ag metal particles have been prepared by sol-gel method. Ag particles are known to exhibit optical absorption at wavelengths around 400 nm when embedded in oxide glasses. Formation of Ag metal particles in TiO$_2$ gel matrix was observed and optical absorption of the composite coating films was measured.

2. EXPERIMENTAL

2.1 Preparation

Titanium tetraisopropoxide, Ti(OC$_3$H$_7$^{i})$_4$, and silver nitrate, AgNO$_3$, were used as the source of TiO$_2$ and Ag, respectively. Firstly, Ti(OC$_3$H$_7$^{i})$_4$ and AgNO$_3$ solutions of various compositions as listed in Table 1 were prepared in order to examine whether or not they are obtained as clear, homogeneous solutions. As shown in the table, homogeneous solutions were

Table 1. Compositions of solutions.

| Soln. No. | Molar ratio | | | | | | | | | | Appearance of solutions |
	Ti(OC$_3$H$_7$^{i})$_4$	AgNO$_3$	H$_2$O	C$_2$H$_5$OH	i-C$_3$H$_7$OH	HNO$_3$	CH$_3$COOH	AcAc	MEA	DEA	
1.	1	0.062	1	8		0.27					Opaque
2.	1	0.062	2	8		0.5					Opaque
3.	1	0.062	1	8			0.1				Opaque
4.	1	0.062	4		8		1				Precipitation
5.	1	0.062	1	8				0.1			Opaque
6.	1	0.062	2		8			1			Precipitation
7.	1	0.062	8		16			1			Transparent
8.	1	0.062	2	8					2		Precipitation
9.	1	0.062	2	8						1.5	Transparent
10.	1	0.062	2		18					1	Transparent
11.	1	0.062	4		18					1	Transparent

AcAc: acetylacetone, MEA: monoethanolamine, DEA: diethanolamine
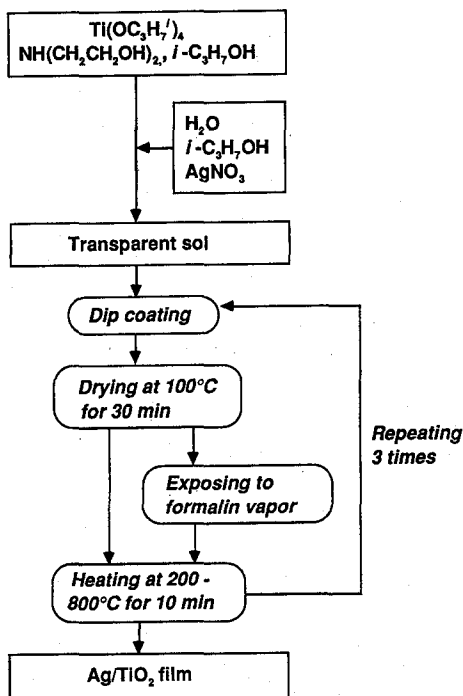
Fig. 1. Flow chart showing the procedure for preparing the coating films.

obtained in Ti(OC$_3$H$_7^i$)$_4$–AgNO$_3$–H$_2$O–i-C$_3$H$_7$OH–CH$_3$COCH$_2$COCH$_3$ and Ti(OC$_3$H$_7^i$)$_4$–AgNO$_3$–H$_2$O–i-C$_3$H$_7$OH (or C$_2$H$_5$OH)–NH(CH$_2$CH$_2$OH)$_2$ solutions.   Addition of acetic acid, which is often used in titanium alkoxide sol-gel systems as an chelating agent for stabilizing the alkoxides against rapid hydrolysis, resulted in formation of opaque solutions, probably because of the precipitation of silver acetate.   In the present work, a solution of molar compositions, Ti(OC$_3$H$_7^i$)$_4$: AgNO$_3$: H$_2$O : i-C$_3$H$_7$OH : NH(CH$_2$CH$_2$OH)$_2$ = 1 : 0.062 : 2 : 18 : 1 was employed for preparation of the coating films.   The molar ratio AgNO$_3$/Ti(OC$_3$H$_7^i$)$_4$ of 0.062 corresponds to a volume fraction of Ag metal of 0.03 in the final Ag/TiO$_2$ composite on the assumption that all Ag and Ti species are converted to Ag metal and TiO$_2$, respectively, and the composite is fully dense.

The flow chart showing the procedure for preparing coating films is illustrated in Fig. 1. AgNO$_3$–H$_2$O–i-C$_3$H$_7$OH solution was added dropwise to Ti(OC$_3$H$_7^i$)$_4$–NH(CH$_2$CH$_2$OH)$_2$–i-C$_3$H$_7$OH solution under vigorous stirring at 0°C.   The resulting clear solution was kept in a sealed beaker at −25°C in a refrigerator for 1 day.   The solution was then warmed to room temperature and used as the coating solution.   A cleaned silica glass substrate was dipped into the solution and vertically withdrawn at a constant rate of 3 cm/min.   The resulting amorphous gel film was dried at 100°C for 30 min and then was heated at 200~800°C for 10 min.   For some of the samples, the gel films were exposed to formalin vapor at room temperature for 30 min prior to the heat-treatment.   This series of procedure was repeated 3 times as shown in Fig. 1.

2.2   Characterization

X-ray diffraction (XRD) of the coating films was measured using a Rigaku RAD II X-ray

diffractometer with Cu Kα radiation operated at 40 kV and 40 mA. For some of the samples, XRD was measured by a Rigaku RINT 1400 diffractometer equipped with a Rigaku CN2651A2 thin-film attachment using Cu Kα radiation operated at 40 kV and 200 mA. For the latter measurement, the glancing angle of the incident beam against the surface of the coating film was fixed at 1°. Scanning rates of 2 or 0.25 deg./min were used in the XRD measurements.

X-ray photoelectron spectroscopy (XPS) measurement was performed using a ULVAC-PHI 5500 spectrometer with Mg Kα radiation operated at 15 kV and 27 mA. Microstructure of the samples was observed by a Hitachi HU-11D transmission electron microscope (TEM) with an acceleration voltage of 75 kV. The thickness of the coating films was evaluated by observing the fracture surface of the sample with a Hitachi S-450 scanning electron microscope. Optical absorption spectra of the coating films were measured by a Hitachi U-3500 spectrophotometer using a silica glass substrate as a reference sample.

3. RESULTS

3.1 X-Ray Diffraction Patterns

The gel film exhibited intense yellow color when exposed to formalin vapor. Fig. 2 shows XRD patterns of the gel coating films before and after formalin vapor exposure. The measurement was carried out using the RINT 1400 diffractometer equipped with the thin film attachment and a scanning rate of 0.25 deg./min. Ag (111) peak is observed at a diffraction angle 2θ around 38° after formalin vapor exposure, while not observed in that without the exposure, indicating that Ag metal particles are formed in the gel film via reduction of Ag^+ ions
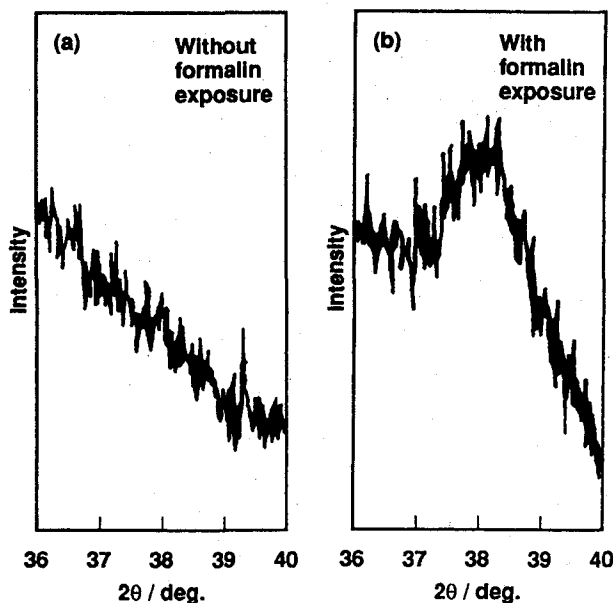

Fig. 2. XRD patterns of the gel films before (a) and after (b) formalin vapor exposure. The X-ray diffractometer equipped with a thin-film attachment was used in the measurement. Cu Kα radiation was operated at 40 kV and 200 mA and a scanning rate of 0.25 deg./min was employed.
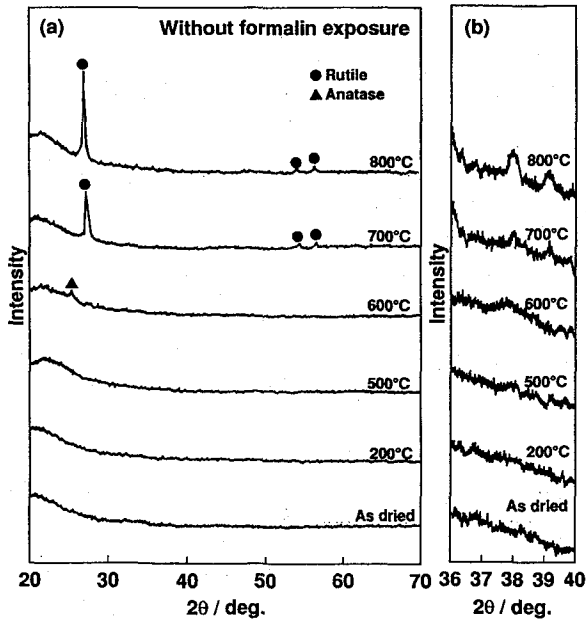
Fig. 3. XRD patterns of the coating films that were obtained by heating the gel films at various temperatures. Cu Kα radiation operated at 40 kV and 40 mA was used. Scanning rates of 2 (a) and 0.25 deg./min (b) were employed.
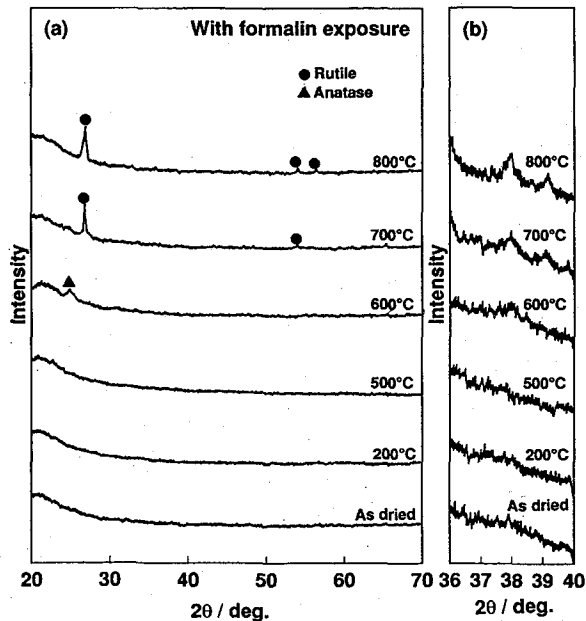

Fig. 4. XRD patterns of the coating films that were obtained by heating the formalin vapor exposed gel films at various temperatures. Cu Kα radiation operated at 40 kV and 40 mA was used. Scanning rates of 2 (a) and 0.25 deg./min (b) were employed.

by formaldehyde.

Fig. 3(a) and 4(a) show XRD patterns of the heat-treated coating films prepared without and with formalin vapor exposure prior to heat-treatment, respectively. The RAD II diffractometer and a scanning rate of 2 deg./min were used in the measurement. It is seen that TiO_2 is crystallized as anatase at 600°C and rutile at 700 and 800°C. Fig. 3(b) and 4(b) show XRD patterns measured at a slower scanning rate of 0.25 deg./min in a limited 2θ range of 36～40°. Ag (111) peak at around $2\theta=38°$ is observed in the samples heated at 600～800°C. In the case of the samples heated at 600°C, however, Ag (111) peak is overlapped with TiO_2 (anatase) (004) peak. XRD peaks are more clearly seen in Fig. 5, where XRD patterns of the heat-treated samples prepared without formalin vapor exposure are shown, which were measured with the RINT 1400 diffractometer with the thin film attachment and a scanning rate of 2 deg./min. A small and broad Ag(200) peak is observed at 2θ around 44°, which is overlapped with TiO_2 (rutile) (210) peak. Considering that, however, on the basis of the literature data TiO_2 (rutile) (210) peak is only 12% of the strongest peak (101) in intensity, which is slightly observed in Fig. 5, contribution of TiO_2 (rutile) (210) peak to the observed peak around 44° can be said to be extremely small. These suggest formation of Ag metal in the samples heated at 600°C.
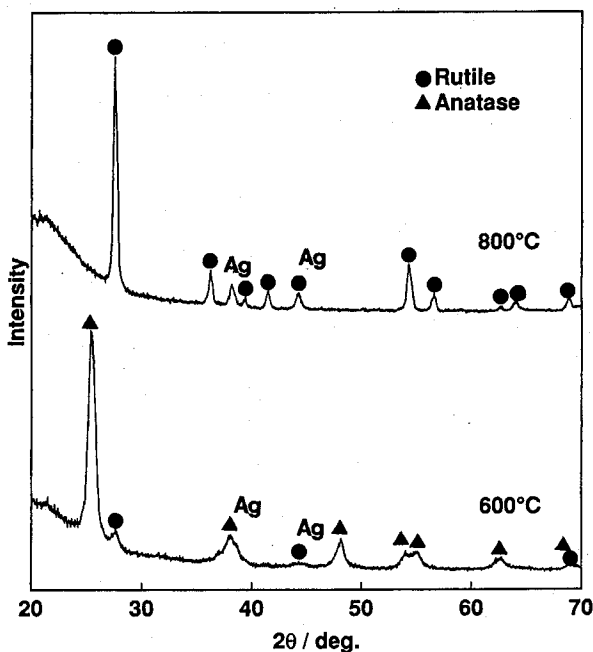

Fig. 5. XRD patterns of the coating films that were obtained by heating the gel films at 600 and 800°C measured using the thin-film attachment, Cu Kα radiation operated at 40 kV and 200 mA and a scanning rate of 2 deg./min.

3.2 XPS Spectra

Fig. 6 shows XPS spectra of Ag 3d and Ti 2p of the coating films heat-treated at 600 and 800°C without formalin vapor exposure. Calibration with the C 1s peak at 284.6 eV resulted in
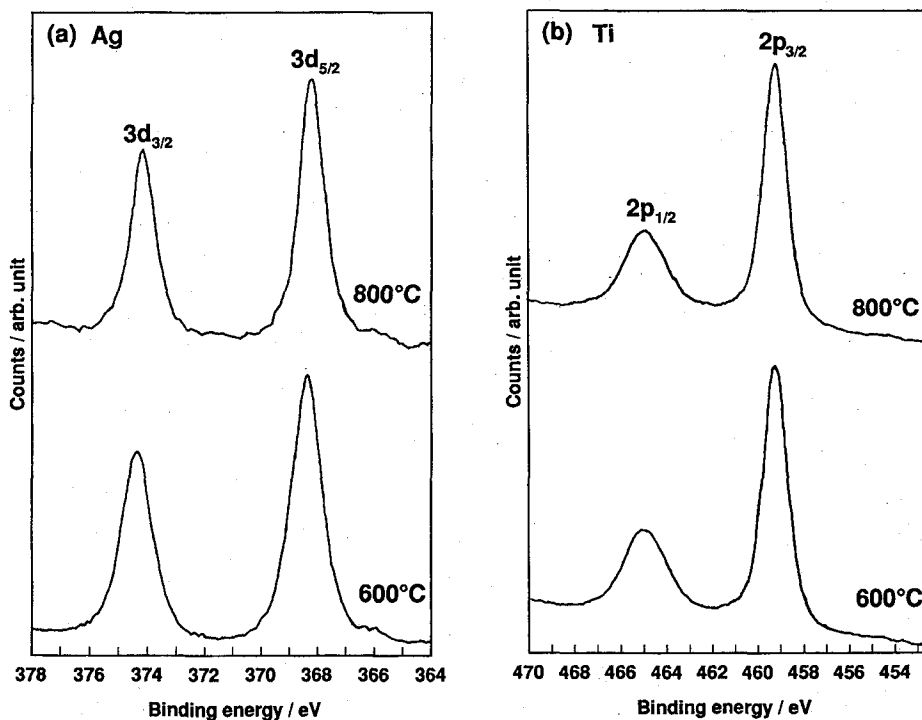
Fig. 6. XPS spectra of Ag 3d (a) and Ti 2p (b) of the coating films that were obtained by heating the gel films at 600 and 800°C. The spectra are calibrated with Ti 2p peak at 459.2 eV.

extremely unreasonable values of binding energies of Ag 3d and Ti 2p peaks probably because of the adsorption of unknown carbon compounds on the sample surfaces. Therefore, the spectra were calibrated with Ti 2p peak at 459.2 eV. The binding energies of Ag 3d$_{5/2}$ were found to be 368.1 and 368.3 eV for the samples heated at 600 and 800°C, respectively (Fig. 6(a)), which agree well with literature data of Ag metal, 368.2 eV.[14-16] The binding energy of Ag$^+$ is reported in ref. 14~16 to be 0.4~0.7 eV lower than that of Ag^0. Contribution of such lower energy peaks is not seen in the present spectra, indicating that all Ag species are present as metal in these samples.

The binding energy of Ti^{3+} is reported to be 1.5 eV lower than that of Ti^{4+}.[17] Contribution of such lower energy peaks is absent in the present Ti 2p spectra, suggesting that there are no reduced Ti species in the samples.

3.3 Optical Absorption Spectra

Fig. 7 and 8 show optical absorption spectra of the heat-treated coating films obtained without and with formalin vapor exposure prior to the heat-treatment, respectively. Small peaks and valleys or waves observed on the spectra are attributed to interference of light. Interference peaks and valleys appeared with much lower frequency in the samples heat-treated at 600~800°C than those non-heated and heated at 200°C. This is due to the smaller film thickness in the heat-treated films, which results from thermal densification. In the gel film exposed to formalin vapor (Fig. 8(a)), an absorption peak at 441 nm, which is attributed to
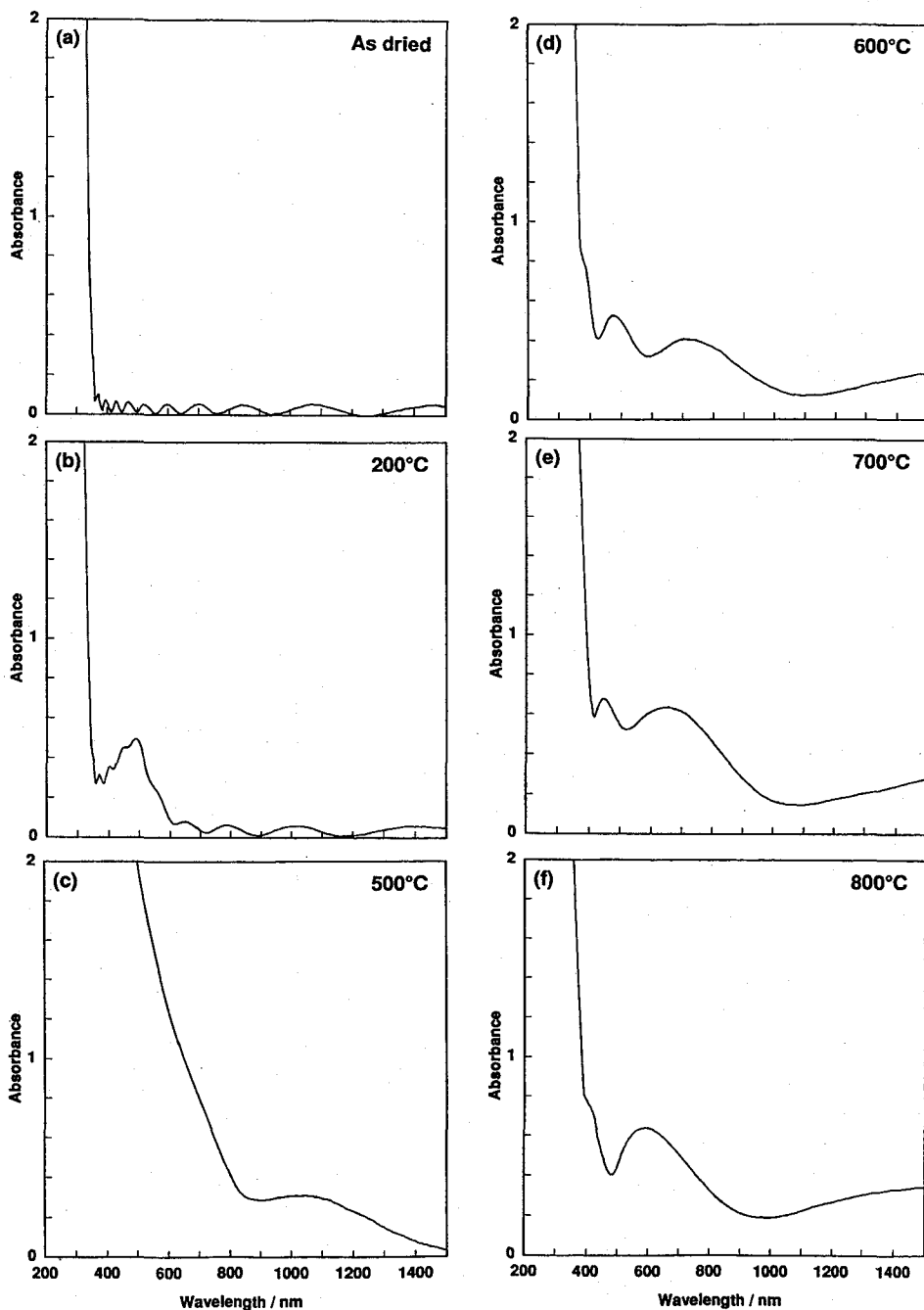
Fig. 7. Optical absorption spectra of the heat-treated coating films prepared without formalin vapor exposure.

surface plasma resonance of Ag metal particles, is observed, while no absorption is seen in the gel film that was not exposed to formalin vapor (Fig. 7(a)). An absorption peak at 466 nm is also seen in the sample that was prepared without formalin vapor exposure and heated at 200°C (Fig.
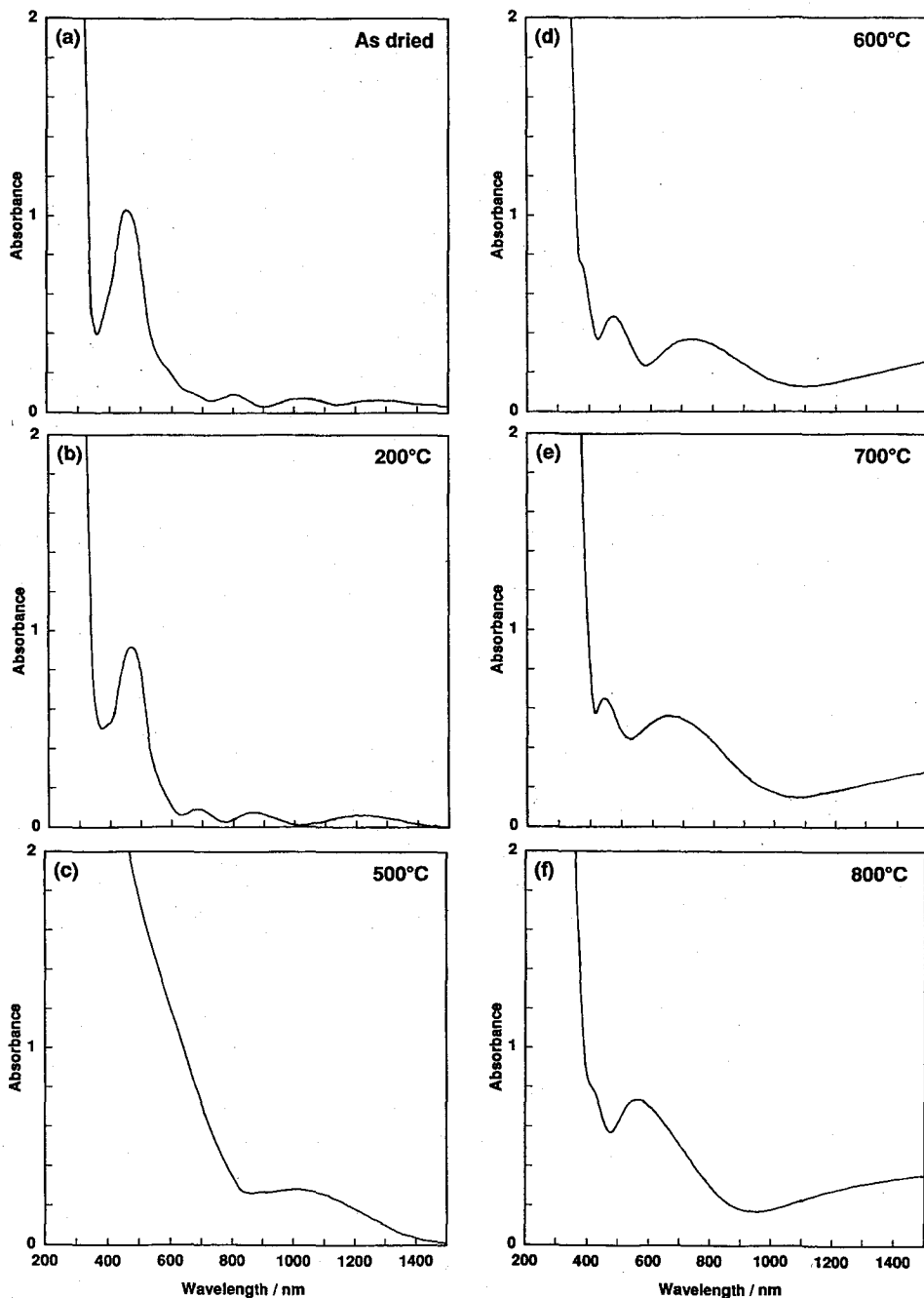
Fig. 8. Optical absorption spectra of the heat-treated coating films prepared with formalin vapor exposure.

7(b)). XRD peaks attributed to Ag metal, however, could not be seen in measurements with RINT 1400 with the thin film attachment. Therefore, the absorption peak cannot be ascribed to surface plasma resonance of Ag metal particles. Thermally decomposed organic substances are

possible origin of the absorption.

Heat-treatment at a higher temperature of 500°C resulted in broad and intense absorption ranging from ultraviolet to about 800 nm (Fig. 7(c) and 8(c)), which is probably due to decomposed carbon species. These intense absorption tails diminished when the samples were heated at a higher temperature of 600°C (Fig. 7(d) and 8(d)) because of the oxidation of the decomposed carbon species. In the samples heated at 600~800°C (Fig. 7(d)~(f) and Fig. 8(d)~(f)) broad absorption bands are observed ranging from ultraviolet to about 1,000 nm, overlapping with two or three interference peaks and valleys. It should be noted that the formalin vapor exposure did not affect the spectra of the samples that were heat-treated at 600~800°C.
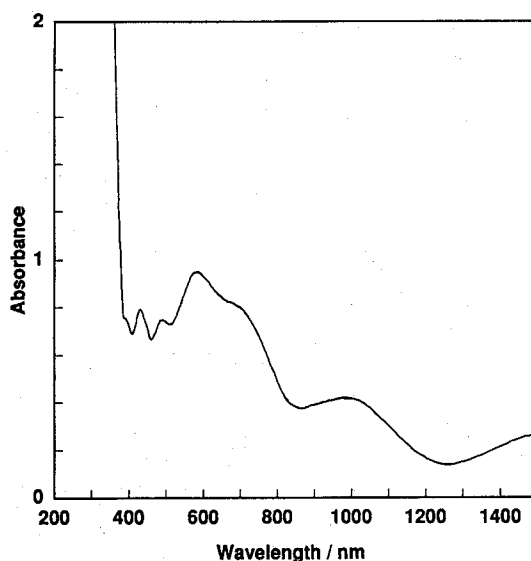

Fig. 9. Optical absorption spectra of a sample obtained by heating the gel film at 600°C for 30 min after drying and exposing to formalin vapor and repeating the coating 5 times.

Fig. 9 shows the absorption spectra of a sample obtained by heating the gel film at 600°C for a longer time of 30 min after drying and exposing to formalin vapor and repeating coating 5 times. The thickness of the film was 0.4 μm, which is larger than that of the sample shown in Fig. 8(d), 0.26 μm. In this case a solution was employed for dip-coating just after being taken out of the refrigerator; the viscosity of the solution should be higher because of its lower temperature. An absorption band peaking at around 580 nm is clearly seen along with the interference peaks and valleys. Higher frequency of the interference peaks and valleys than those observed in Fig. 8(d) is due to the larger film thickness.

3.4 TEM Observation

TEM pictures of the gel coating films are shown in Fig. 10. The TEM pictures revealed presence of Ag metal particles of 4~23 nm in size in the dried gel coating films that were exposed to formalin vapor (Fig. 10(b)). Such particles could not be found in the gel films that were not
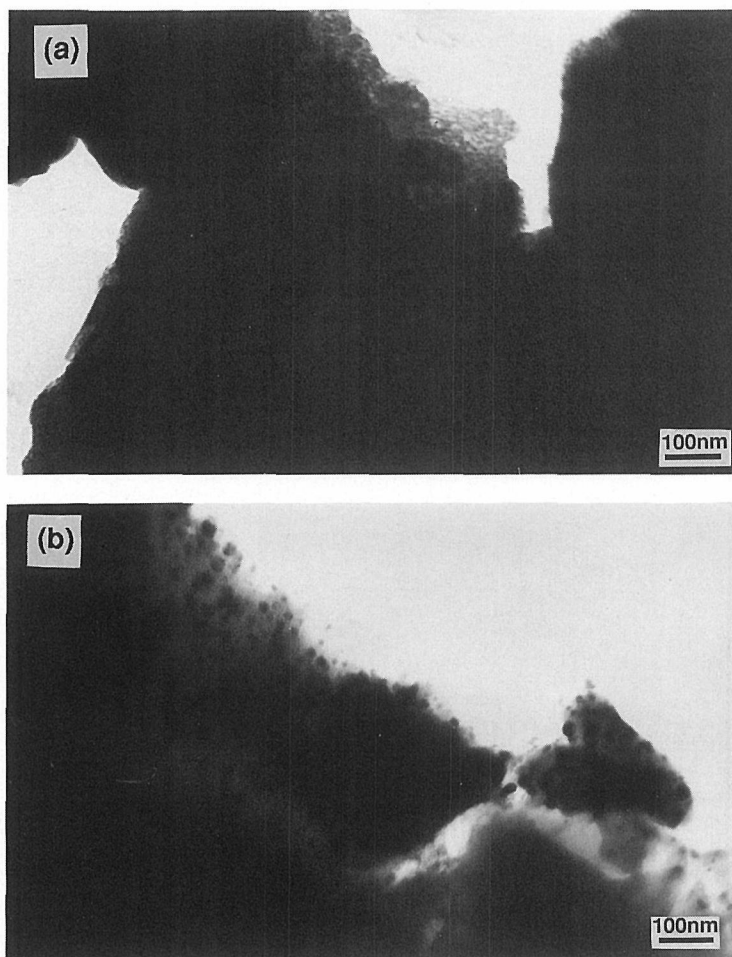
Fig. 10. TEM pictures of the gel coatings films before (a) and after (b) formalin vapor exposure.

exposed to formalin vapor (Fig. 10(a)).

Fig. 11 shows TEM pictures of the samples heated at 600°C. Fig. 11(a) and (b) show TEM pictures of the samples prepared without and with formalin vapor exposure, respectively. The sample shown in Fig. 11(c) was prepared by heating the formalin vapor exposed gel film at 600°C for 30 min with 5 times repeated coatings. Namely, the samples shown in Fig. 11(a), (b) and (c) *correspond to those whose optical absorption spectra have been shown in Fig. 7(d), Fig. 8(d) and* Fig. 9, respectively. Ag metal particles of 5～25 nm were observed in these samples. Negligible difference was found between the samples prepared with and without formalin vapor exposure.

Fig. 12 shows TEM pictures of the samples heated at 800°C without and with formalin vapor exposure. Ag particles of 13～41 nm and 13～45 nm were observed in the samples prepared without and with the formalin vapor exposure, respectively. It should be noted that both Ag particles and TiO₂ crystals are larger in size in the samples heated at 800°C than those at 600°C.
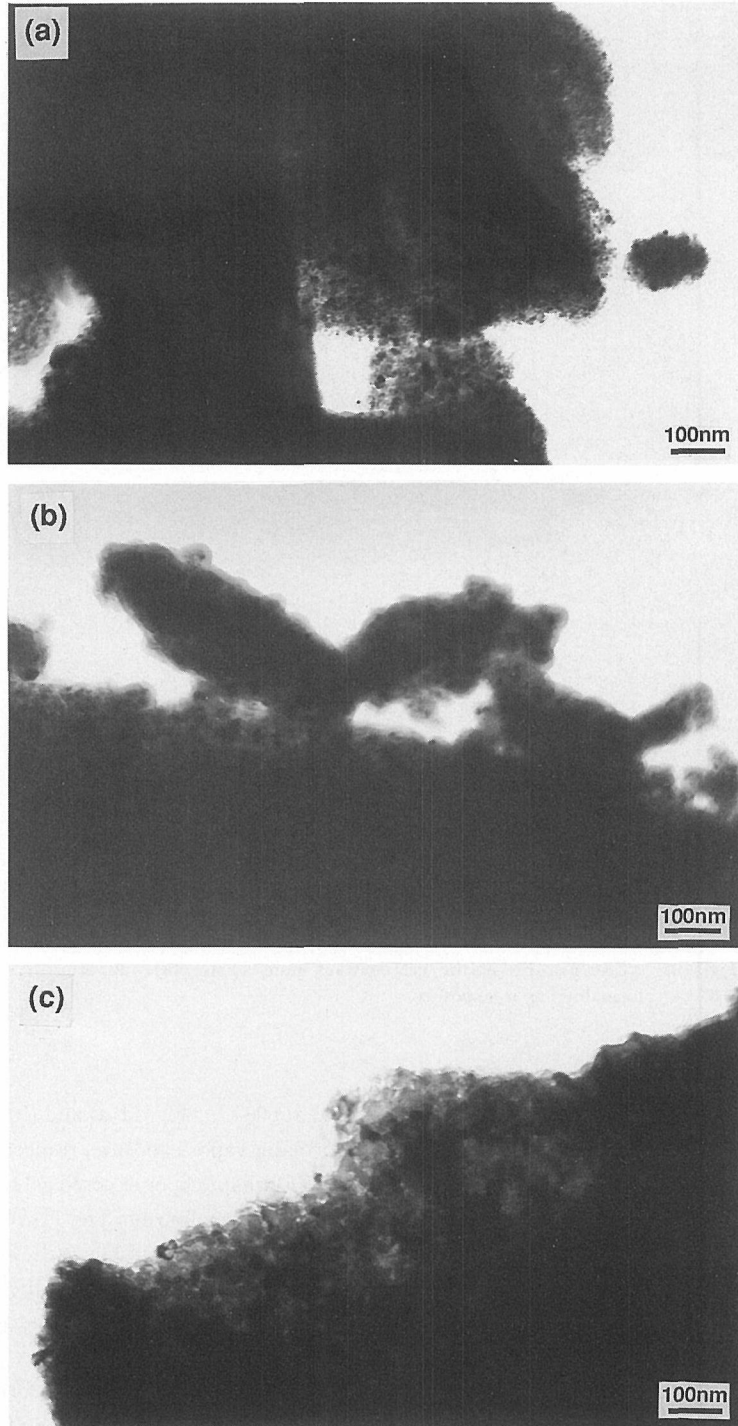
Fig. 11. TEM pictures of the coating films heat-treated at 600°C. (a) Without formalin vapor exposure. (b) With formalin vapor exposure. (c) Corresponding to the sample shown in Fig. 9.
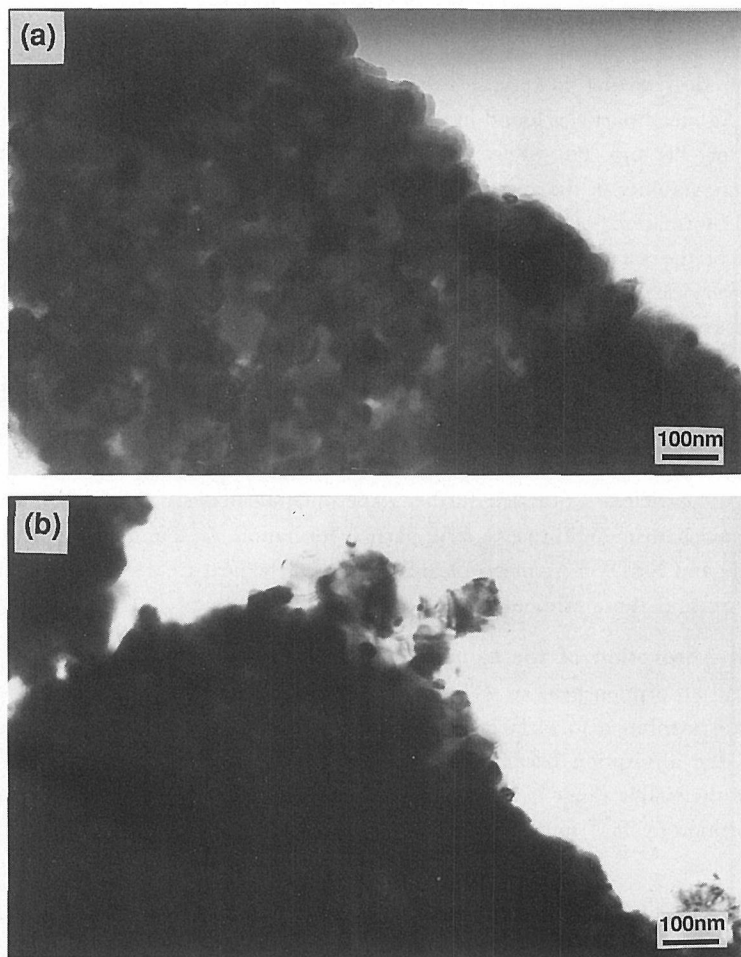
Fig. 12. TEM pictures of the coating films heat-treated at 800°C. (a) Without formalin vapor exposure. (b) With formalin vapor exposure.

4. DISCUSSION

4.1 Formation of Ag Metal Particles in the Coating Films

Exposure to formalin vapor caused reduction of Ag$^+$ ions and formation of nanometer-sized Ag metal particles in the gel films. Considering the high concentration of Ag$^+$ ions in the starting solution, 0.034 mol/l, formation of nanometer-sized Ag metal particles cannot be expected if reduction is carried out in solutions; instead aggregation of Ag particles would occur, and formation of much larger Ag particles and precipitation would take place in solutions. It is thought that Ag$^+$ ions trapped in the titania gel pores were reduced and Ag metal particles were formed within the gel pores, where migration of Ag ions, atoms or particles is much more limited than in solutions.

It has been found that temperatures as high as 600°C were needed for formation of Ag metal particles when the gel films that were not exposed to formalin vapor were heat-treated in air. In

our previous studies,[9~11,18] metal particle formation in gel films were found to occur at about 200°C for Au, 800°C for Pt and 900°C for Pd, where $HAuCl_4 \cdot 4H_2O$, $H_2PtCl_6 \cdot 6H_2O$ and $PdCl_2$ were used as the starting materials, respectively. Therefore the temperature needed for formation of Ag metal particles found in the present study is higher than that for Au and lower than those for Pt and Pd. This order of temperatures roughly agrees with that of thermodynamic stability of the corresponding oxides against reduction. The temperature for metal particle formation, of course, is also affected by the kinds of raw materials and the compositions of the starting solutions and gel films.

It is not very clear whether or not the Ag particles formed at room temperature by formalin vapor exposure remained as they were when the films were heated at 600°C. At least the size of Ag particles was almost unchanged, while the change in the amount of Ag metal particles is not ·clear. When the gel films exposed to formalin vapor were heated at 800°C, Ag particles larger in size than at 600°C were formed. Formation of larger Ag particles is thought to occur via (1) growth of Ag particles by consuming Ag atoms that have not been crystallized, or (2) Ostwald ripening of Ag particles. Although further experimental analysis should be carried out to elucidate the mechanism and process of Ag particle formation, we found negligible difference in microstructure and XRD on Ag metal particles between the heat-treated samples with formalin vapor exposure and those without it.

4.2 Optical Absorption of the Composite Coating Films

An optical absorption peak at 441 nm was observed in the gel films exposed to formalin vapor, which is attributed to surface plasma resonance of Ag particles. When the films were heat-treated, the absorption became broad and shifted to longer wavelengths. The broad absorption in the visible range is attributed to surface plasma resonance of Ag metal particles. Optical absorption by Ti^{3+} ions can be ruled out because Ti^{3+} was not detected in Ti 2p XPS
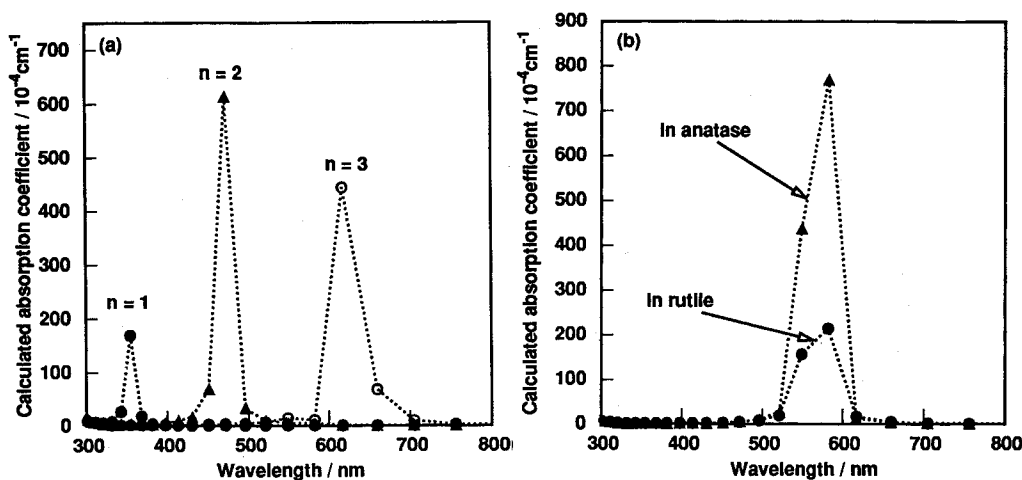

Fig. 13. Absorption curves calculated with eq. (1) for Ag particles dispersed in dielectric media of various refractive indices (a) and in anatase and rutile (b). In calculation in (b), α was calculated in a way that $\alpha = (\alpha_O + 2\alpha_E)/3$, where α_O and α_E are absorption coefficients calculated using dielectric constants for ordinary and extraordinary rays, respectively. p was assumed to be 0.03 in the calculation.

spectra. According to Mie theory,[19] the optical absorption coefficient, $\alpha(\lambda)$, of metal nanoparticles/dielectric media composites is related to the dielectric constants of metal and dielectric media, $\varepsilon_m(\lambda) = \varepsilon_m{}'(\lambda) + i\varepsilon_m{}''(\lambda)$, and $\varepsilon_d(\lambda)$, respectively, as follows;

$$\alpha(\lambda) = \frac{18\pi p \varepsilon_d(\lambda)^{3/2}}{\lambda} \frac{\varepsilon_m{}''(\lambda)}{(\varepsilon_m{}'(\lambda) + 2\varepsilon_d(\lambda))^2 + \varepsilon_m{}''(\lambda)^2} \tag{1}$$

where p is the volume fraction of the metal particles and λ is the wavelength of light. The effects of the particle size and shape are not taken into account in this equation. Fig. 13 (a) shows optical absorption curves calculated with eq. (1) for Ag particles that are dispersed in dielectric media of refractive indices n of 1, 2 and 3, or $\varepsilon_d(\lambda)$ of 1, 1.41, 1.73. It is seen that the absorption peak shift from about 350 to 610 nm when n is increased from 1 to 3. Therefore, the shift of the absorption band to longer wavelengths can be explained in terms of the increase in the dielectric constant or refractive index of the titania medium, which results from thermal densification and crystallization. Fig. 13(b) shows absorption curves calculated with eq. (1) for Ag particles that are dispersed in anatase and rutile. These curves have peaks at around 580 nm, which roughly agrees with the absorption peak observed in Fig. 9. In these calculations, literature data on $\varepsilon_m{}'(\lambda)$ and $\varepsilon_m{}''(\lambda)$ for Ag[20] and $\varepsilon_d(\lambda)$ for anatase[21] and rutile[22] were used and p was assumed to be 0.03.

The heat-treated samples showed much broader absorption peaks than the gel film exposed to formalin vapor. Papavassiliou[19] has pointed out that in general the absorption band of metal particles become broader when the dielectric constant of the surrounding medium is increased. Therefore, the increased dielectric constant of titania phase caused by thermal densification and crystallization is a possible source of the broadening of the absorption peak of the sample heated at 600°C. It is also described in ref. 19 that larger metal particles show broader absorption peaks as well as peaks at longer wavelengths. This is not, however, the case with the present sample heated at 600°C compared with the gel film exposed to formalin vapor. Another possible source of the broadening of the absorption peaks is larger distribution in particle size and shape, for which further experimental analysis should be made more in detail. Preparation of TiO$_2$ films containing smaller Ag particles with narrower size distribution, however, would be expected to exhibit sharper optical absorption peaks.

5. CONCLUSIONS

TiO$_2$ coating films containing dispersed, nanometer-sized Ag metal particles have been prepared by the sol-gel method. Exposure of the gel film to formalin vapor at room temperature caused reduction of Ag$^+$ ions and formation of Ag metal particles of 4~23 nm in size in the gel film. Heat-treatment of the gel films at 600~800°C in air resulted in formation of anatase or rutile polycrystalline films containing Ag metal particles of 5~45 nm in size, whether or not the gel films were exposed to formalin vapor prior to heat-treatment. Because of the increase in dielectric constant of the oxide phase, which is caused by thermal densification and crystallization, the absorption peak due to surface plasma resonance of Ag metal particles shifted to longer wavelengths when the films were heat-treated.

REFERENCES

(1) A. Wokaun, *Mol. Phys.*, **56**, 1 (1985).

(2) D. Ricard, Ph. Roussignol and Chr. Flytzanis, *Opt. Lett.*, **10**, 511 (1985).

(3) R. Reisfeld, M. Eyal and D. Brusilovsky, *Chem. Phys. Lett.*, **153**, 210 (1988).

(4) A. Hinsch, A. Zastrow and V. Witter, *Solar Energy Mater.*, **21**, 151 (1990).

(5) H.R. Wilson, *Solar Energy Mater.*, **16**, 223 (1987).

(6) O.L. Malta and M.A. Couto dos Santos, *Chem. Phys. Lett.*, **174**, 13 (1990).

(7) J. Matsuoka, R. Mizutani, S. Kaneko, H. Nasu, K. Kamiya, K. Kadono, T. Sakaguchi and M. Miya, *J. Ceram. Soc. Jpn.*, **101**, 53 (1993).

(8) H. Kozuka and S. Sakka, *Chem. Mater.*, **5**, 222 (1993).

(9) H. Kozuka, G. Zhao and S. Sakka, *J. Sol-Gel Sci. Techn.*, **2**, 741 (1994).

(10) P. Innocenzi, H. Kozuka and S. Sakka, "*J. Sol-Gel Sci. Techn.*, **1**, 305 (1994).

(11) G. Zhao, H. Kozuka and S. Sakka, *J. Sol-Gel Sci. Techn.*, in press.

(12) C.-Y. Li, J.Y. Tseng, C. Lechner and J.D. Mackenzie, *Mat. Res. Soc. Symp. Proc.*, **272**, 133 (1992).

(13) L. Spanhel, M. Mennig and H. Schmidt, in Proceedings of the XVIIth International Congress on Glass, Vol. 7, p. 9 (1992).

(14) J.S. Hammond, S.W. Gaarenstroom and N. Winograd, *Anal. Chem.*, **47**, 2194 (1975).

(15) S.W. Gaarenstroom and N. Winograd, *J. Chem. Phys.*, **67**, 3500 (1977).

(16) G. Schoen, *Acta Chem. Scand.*, **27**, 2623 (1973).

(17) T. Choudhury, S.O. Saied, J.L. Sullivan and A.M. Abbot, *J. Phys. D : Appl. Phys.*, **22**, 1185 (1989).

(18) H. Kozuka, T. Toyoshima and S. Sakka, to be submitted.

(19) G.C. Papavassiliou, *Prog. Solid State Chem.*, **12**, 185 (1979).

(20) P.B. Johnson and R.W. Christy, *Phys. Rev. B*, **6**, 4370 (1972).

(21) *International Critical Tables of Numerical Data, Physics, Chemistry and Technology*, ed. by E.W. Washburn, National Research Council of the United States of America, p. 19 (1929).

(22) J.R. DeVore, *J. Opt. Amer.*, **41**, 416 (1951).